

ISSN: 0256-307X

# 中国物理快报

# Chinese Physics Letters

Volume 32 Number 10 October 2015

A Series Journal of the Chinese Physical Society  
Distributed by IOP Publishing

Online: <http://iopscience.iop.org/0256-307X>  
<http://cpl.iphy.ac.cn>

CHINESE PHYSICAL SOCIETY  
**IOP** Publishing

JUST FOR AUTHORS  
— CHINESE PHYSICS LETTERS

## Fabrication of Through Micro-hole Arrays in Silicon Using Femtosecond Laser Irradiation and Selective Chemical Etching \*

GAO Bo(高博), CHEN Tao(陈涛)\*\*, CHEN Ying(陈颖), SI Jin-Hai(司金海), HOU Xun(侯洵)

Key Laboratory for Physical Electronics and Devices of the Ministry of Education & Shaanxi Key Lab of Information Photonic Technique, School of Electronics & information Engineering, Xi'an Jiaotong University, Xi'an 710049

(Received 24 May 2015)

*We demonstrate a method of fabricating through micro-holes and micro-hole arrays in silicon using femtosecond laser irradiation and selective chemical etching. The micro-hole formation mechanism is identified as the chemical reaction of the femtosecond laser-induced structure change zone and hydrofluoric acid solution. The morphologies of the through micro-holes and micro-hole arrays are characterized by using scanning electronic microscopy. The effects of the pulse number on the depth and diameter of the holes are investigated. Honeycomb arrays of through micro-holes fabricated at different laser powers and pulse numbers are demonstrated.*

PACS: 79.20.Eb, 79.20.Ws, 82.30.-b

DOI: 10.1088/0256-307X/32/10/107901

Silicon plays an important role in micro-electro-mechanical systems and microelectronic devices, and dominates the optoelectronics industry. Among various silicon processing techniques, through silicon via technology has attracted wide attention owing to its application in the packaging of semiconductor devices and the fabrication of through micro-hole arrays.<sup>[1-3]</sup> The most important application of through micro-hole arrays is silicon microchannel plates, which have provided the basic structures of photomultipliers for weak signal amplification.<sup>[4-6]</sup> Compared with traditional glass microchannel plates, silicon microchannel plates have drawn much attention due to their strong advantages, such as low noise, high-temperature-compatible processing, long-term stability, and potentially much more space for gain improvement.<sup>[7]</sup> Silicon microchannel plates are also an important candidate for anodes of three-dimensional batteries.<sup>[8,9]</sup>

A combined system including lithography and reactive-ion etching<sup>[10]</sup> is generally used to pattern silicon.<sup>[11]</sup> However, the low processing rate, necessity for micro-masks in the etched field, and processing complexity are the main drawbacks of these methods. Femtosecond laser direct writing has been employed as a powerful method of micromachining various materials.<sup>[12-16]</sup> Compared with conventional methods, it has many notable advantages for laser micromachining such as noncontact processing, fast removal rates, and freedom from etch masks.<sup>[17]</sup> Many studies have been carried out on femtosecond laser drilling micro-holes in silicon.<sup>[18,19]</sup> However, debris is generated during the laser ablation process, which blocks energy delivery to deeper regions of the silicon and makes it difficult to increase the hole depth.

We recently found that a femtosecond laser could produce buried microchannels in silicon. It was also found that oxygen can be incorporated into silicon when it is irradiated by a femtosecond laser in air.<sup>[20]</sup> The femtosecond-laser-induced oxygen doping zones extend from the silicon surface into the interior and could be very deep and of high aspect ratio. After removing silicon oxide in the laser-induced structure change (LISC) zones, we may fabricate high-aspect-ratio structures.

In this work, we demonstrate a method of fabricating through micro-holes and micro-hole arrays in silicon by combining femtosecond laser irradiation and selective chemical etching. An 800-nm femtosecond laser is employed to induce LISC in silicon. Then, selective chemical etching with a hydrofluoric (HF) acid solution is used to remove the materials in the LISC zones to form micro-holes. Scanning electronic microscopy (SEM) is employed to characterize the morphologies of the micro-holes and micro-hole arrays. The elements' characterization is carried out with an energy dispersive x-ray spectroscopy (EDS, TEAMTM Serials). The micro-hole formation mechanism is identified as the chemical reaction of the silicon oxide in LISC zones and HF acid solution. Furthermore, honeycomb arrays of micro-holes fabricated at different laser powers and pulse numbers are demonstrated.

The experimental setup consists of a femtosecond laser source, an attenuator, a neutral density filter, a mechanical shutter, an *xyz* movable stage, a computer, and a charge-couple device (CCD) camera. In the experiment, the laser source was an amplified Ti:sapphire femtosecond laser system (Libra-USP-HE,

\*Supported by the National Basic Research Program of China under Grant No 2012CB921804, the National Natural Science Foundation of China under Grant Nos 11204236 and 61308006, and the Collaborative Innovation Center of Suzhou Nano Science and Technology.

\*\*Corresponding author. Email: tchen@mail.xjtu.edu.cn

© 2015 Chinese Physical Society and IOP Publishing Ltd

Coherent Co., USA), which delivered a 1-kHz pulse train with a pulse duration of 50 fs and central wavelength of 800 nm. The attenuator provided a convenient way to adjust the laser power, and the mechanical shutter was employed to control the laser beam access. Samples were mounted on a movable stage with high precision. The motion of the stage was controlled by a computer program. The CCD camera was connected to a computer for real-time observation of the sample surface during fabrication.

A 1-cm<sup>2</sup> square silicon wafer 280  $\mu\text{m}$  in thickness was used in our experiments. Firstly, the sample was cleaned in acetone and deionized water by an ultrasonic machine for 15 min each. Subsequently, the sample was mounted on the movable stage. The laser beam was focused onto the sample by a 10 $\times$  microscope objective lens (numerical aperture of 0.3, Nikon). The focus was set on the silicon wafer surface. The accumulated pulse numbers at each spot were controlled by varying the opening time of the mechanical shutter.

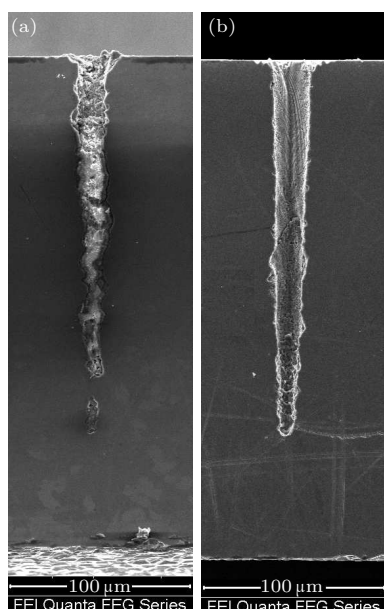
After femtosecond laser irradiation, the silicon sample was cleaned in acetone and deionized water in an ultrasonic bath for 15 min each. Subsequently, the sample was selectively etched with a 20 wt% HF acid solution for 30 min. SEM was employed to characterize the morphologies of the micro-holes and micro-hole arrays. For observing cross-sectional morphologies of micro-holes in silicon, we polished laser-treated samples with an abrasive paper in a direction orthogonal to the surface from one edge of the surface. The sample was polished for a few tens of seconds and then observed under a microscope to check the polished depth. This process was repeated until the polished surface reached the central axial position of micro-holes. Due to the fact that silicon was opaque, it was difficult to make the polished surface just reach the center axial position of a hole. Sometimes the sample was polished over the position. Hence, more than 10 LISC zones were fabricated at the same laser irradiation condition and arranged in honeycomb array with a separation of 200  $\mu\text{m}$ . The polished sample was cleaned in acetone and deionized water in an ultrasonic bath. After cleaning, the sample was characterized with SEM and then etched with HF acid.

Figure 1 illustrates the morphologies of the LISC zone before and after chemical etching. The laser power was set at 45 mW, and the pulse number was set at 2000. In Fig. 1(a), we can see that the LISC was formed in silicon along the femtosecond laser transmission direction in the irradiated zones. According to the EDS analysis, oxygen was doped into the whole LISC zone due to the interaction of femtosecond laser and silicon. The concentration of oxygen decreased with the increase of the LISC depth. The atomic percentage of oxygen was about 42% at the top and decreased

to zero at the end of LISC zone. The micro-hole was not formed due to the existence of silicon oxide in the laser-irradiated region.<sup>[20]</sup> The oxide in LISC zone was hardly removed by acetone and deionized water in an ultrasonic bath, especially for the uncut LISC zones. The silicon sample treated by the femtosecond laser was subsequently etched with an HF acid solution for 30 min. The result is shown in Fig. 1(b). We can see that the oxide in the LISC was completely removed, and a micro-hole was formed in the silicon. The micro-hole had a diameter of about 18  $\mu\text{m}$  and a depth of about 200  $\mu\text{m}$ . The aspect ratio (micro-hole depth divided by hole diameter at the half-depth) was calculated to be about 11. According to the irradiation time and hole depth, the formation rate of the LISC zone in depth was calculated to be 100  $\mu\text{m}/\text{s}$ . After considering the etching time of 30 min, the formation rate of holes in depth was estimated to be about 67  $\mu\text{m}/\text{min}$ . The uncut LISC zones were also cross sectioned by polishing and characterized after etching, and materials in these LISC zones were also removed completely. According to the above results, the silicon oxides in LISC were hardly removed with water and acetone but removed with HF acid. It is well known that the reaction between HF acid and silica oxide is a dissolution reaction. Hence, we believe that the removing of materials in the LISC zone was due to the reaction between silica oxide in LISC zones and HF acid. Note that only the materials in the LISC zone reacted with the HF acid solution, while the surrounding zones remained unchanged. This is due to the fact that HF acid could react with silicon oxide while not with silicon.

We further investigated the effects of the pulse number on the depth and diameter of the holes. The laser power was set at 45 mW, and the pulse number was varied from 100 to 3000. Figure 2(a) shows the evolution of the hole depth and diameter as a function of the pulse number. The depth increases as the pulse number increases, which is attributed to greater accumulation of laser energy in the laser-irradiated region with increasing the pulse number. When the pulse number was increased to 1600, a through micro-hole was fabricated in the 280- $\mu\text{m}$ -thick silicon sample. On the other hand, the hole diameter initially increases slightly as the pulse number increases and then remains almost unchanged as the number of pulses reaches 1600. This is due to the fact that the effective irradiated zones on the material in the plane perpendicular to the light transmission direction depend on the beam size. Figure 2(b) illustrates the dependence of the aspect ratio of the holes on the pulse number, and the insets show the morphologies of three of the corresponding holes. The aspect ratio of the holes increases with the pulse number. This is due to the increase of the depth and the slight increase of the di-

ameter of the silicon holes. The aspect ratios remain unchanged as the number of pulses reaches 1600. The results show that the maximum aspect ratio of the holes is 15.5, at a depth of 280  $\mu\text{m}$  and diameter of 18.1  $\mu\text{m}$ . For the maximum aspect ratio of 15.5, the hole depth of 280  $\mu\text{m}$  reached the thickness of silicon.



**Fig. 1.** Morphology of silicon micro-hole: (a) the LISC zone, (b) after selective chemical etching.

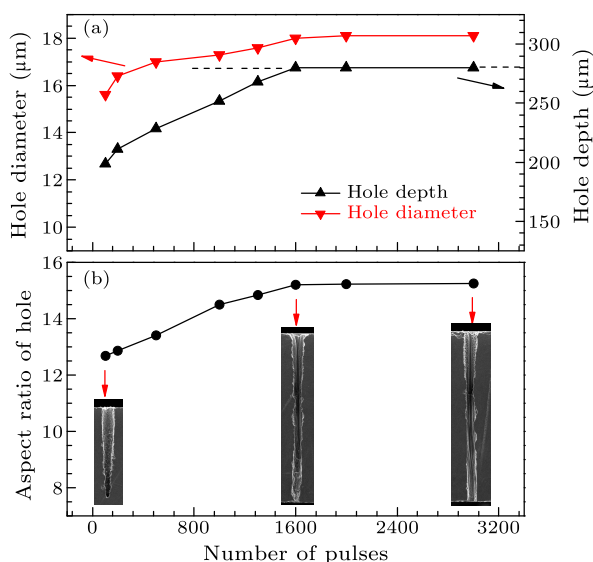


**Fig. 2.** (a) Depths and diameters and (b) aspect ratios of holes versus femtosecond laser pulse number. Dashed line corresponds to the silicon sample thickness. Insets show morphologies of corresponding holes.

As shown in Fig. 2(a), the hole depths linearly increased with pulse numbers when the pulse number was increased over 200. When holes reached the bottom of samples 280  $\mu\text{m}$  in thickness, the increase of hole depths was unsaturated as pulse numbers increased while the hole diameters remain almost un-

changed. Therefore, if a thicker silicon sample is used, depths and aspect ratios of holes would increase further with pulse numbers. The pulse depth and aspect ratio could also be increased by increasing the laser power. In addition, as shown in insets of Fig. 2(b), the hole shows a conical shape at the pulses number of 100. When the numbers of accumulated laser pulses were over 1600, the hole diameters became almost uniform at different depths. Therefore large pulse numbers were needed to obtain the holes with uniform shape.

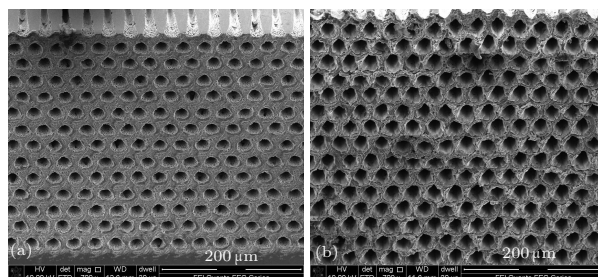


**Fig. 3.** SEM images of honeycomb arrays of micro-holes fabricated by using femtosecond laser irradiation and selective chemical etching. (a) Hole entrances for the sample fabricated at laser power of 30 mW and pulse number of 4000; (b) hole entrances for the sample fabricated at laser power of 45 mW and pulse number of 1600.

Furthermore, honeycomb arrays of micro-holes were fabricated by using femtosecond laser irradiation and selective chemical etching. After laser irradiation, the silicon samples were etched with HF acid solution for 30 min to form through micro-holes. Figure 3 shows the SEM images of micro-hole arrays fabricated at different laser powers and pulse numbers. The distance between neighboring micro-holes was 30  $\mu\text{m}$ . Figure 3(a) shows the hole entrances of micro-hole arrays after selective chemical etching for the sample fabricated at a laser power of 30 mW and the pulse number of 4000. Figure 3(b) shows the hole entrances of micro-hole arrays after selective chemical etching for the sample fabricated at a laser power of 45 mW and the pulse number of 1600. The entrances of the micro-holes were obviously almost circular. The diameters of the entrances of the micro-holes were about 18 and 22  $\mu\text{m}$  for the samples treated at 30 and 45 mW, respectively. The entrances of the holes produced under a low laser power of 30 mW are clean. When the applied laser power was increased to 45 mW, the entrances of the holes show an obvious thermally affected zone. The formation of the thermally affected zone was due to the mixture of molten and vaporized silicon driven up by laser that was partially redeposited on the top surface and around the periphery of the LISC zone. The thermal damage layer usually exists on the surface of the laser ablation region and was very thin (with thickness of a few micrometers).<sup>[21]</sup> Uniform through hole arrays could be attained by polishing the thermally effected layer on the sample sur-

face. In addition, the surfaces of micro-holes were not smooth. The roughness of holes may be decreased by the isotropic etching using a mixed acid solution of hydrofluoric acid, nitric acid, and acetic acid. By using this mixed acid solution, microlenses with smooth surfaces have been attained on the silicon surface.<sup>[22]</sup>

In conclusion, we have demonstrated a method of fabricating through micro-holes and micro-hole arrays in silicon using femtosecond laser irradiation and selective chemical etching. First, LISC is induced in silicon by femtosecond laser irradiation. Second, HF acid solution is employed to remove silicon oxide in the LISC zones to form micro-holes. The morphology of the micro-holes and micro-hole arrays is characterized by using SEM. The dependences of the hole depth and diameter on the pulse number are investigated. Honeycomb arrays of micro-holes fabricated at different laser powers and pulse numbers are demonstrated. This method has potential applications in the fabrication of silicon microchannel plates and other Si-based advanced devices.

The SEM work was performed at the International Center for Dielectric Research (ICDR), Xi'an Jiaotong University, Xi'an, China. The authors also sincerely thank Ms. Dai for her help in the use of SEM.

## References

- [1] Motoyoshi M 2009 *Proc. IEEE* **97** 43
- [2] Liu X X, Zhu Z M, Yang Y T, Wang F J and Ding R X 2014 *Chin. Phys. B* **23** 583
- [3] Dong G, Wu W X and Yang Y T *Acta Phys. Sin.* **64** 026601 (in Chinese)
- [4] Beetz C P, Boerstler R, Steinbeck J, Lemieux B and Winn D R 2000 *Nucl. Instrum. Methods Phys. Res. Sect. A* **442** 443
- [5] Siegmund O H W, Tremsin A S, Vallerga J V, Beetz C P, Boerstler R W, Yang J and Winn D R 2002 *Proc. SPIE* **4497** 139
- [6] Lapington J S, Ashton T J R, Ross D and Conneely T 2012 *Nucl. Instrum. Methods Phys. Res. Sect. A* **695** 78
- [7] Chen X M, Lin J L, Yuan D, Ci P L, Xin P S, Xu S H and Wang L W 2008 *J. Micromech. Microeng.* **18** 037003
- [8] Wang F, Xu S H, Zhu S S, Peng H, Huang R, Wang L W, Xie X H and Chu P K 2013 *Electrochim. Acta* **87** 250
- [9] Yu S J, Luo C H, Wang L W, Peng H and Zhu Z Q 2013 *Analyst* **138** 1149
- [10] Ma X Z, Zhang R, Sun J B, Shi Y and Zhao Y 2015 *Chin. Phys. Lett.* **32** 045202
- [11] Mukherjee P, Zurbuchen T H and Guo L J 2009 *Nanotechnology* **20** 325301
- [12] Tan D Z, Zhou S F, Qiu J R and Khusro N 2013 *J. Photochem. Photobiol. C-Photochem. Rev.* **17** 50
- [13] Qiu J R 2004 *Chem. Rec.* **4** 50
- [14] Wang J L, He B R, Dai S X, Zhu J F and Wei Z Y 2015 *IEEE Photon. Technol. Lett.* **27** 1041
- [15] Matsuo S and Hashimoto S 2015 *Opt. Express* **23** 165
- [16] Wu Q, Xu J J, Zhang G Q, Zhao L J, Zhang X Z, Qiao H J, Sun Q, Lu W Q, Zhang G Y and Volk T R 2003 *Opt. Mater.* **23** 277
- [17] Gattass R R and Mazur E 2008 *Nat. Photon.* **2** 219
- [18] Laakso P, Penttilä R and Heimala P 2010 *J. Laser Micro/Nanoen.* **5** 273
- [19] Ahn S, Hwang D J, Park H K and Grigoropoulos C P 2012 *Appl. Phys. A* **108** 113
- [20] Ma Y C, Pan A, Si J H, Chen T, Chen F and Hou X 2012 *Opt. Commun.* **285** 140
- [21] Coyne E, O'Connor G M, Mannion P, Magee J and Glynn T J 2004 *Proc. SPIE* **5339** 73
- [22] Pan A, Gao B, Chen T, Si J H, Li C X, Chen F and Hou X 2014 *Opt. Express* **22** 15245



# Chinese Physics Letters

Volume 32

Number 10

October 2015

## GENERAL

- 100301 An Efficient Multiparty Quantum-State Sharing Scheme**  
QIN Hua-Wang, DAI Yue-Wei
- 100302 Motion of a Nonrelativistic Quantum Particle in Non-commutative Phase Space**  
FATEME Hoseini, MA Kai, HASSAN Hassanabadi
- 100303 Quantum Correlations in Ising-XYZ Diamond Chain Structure under an External Magnetic Field**  
Faizi E., Eftekhari H.
- 100401 On Hawking Radiation of 3D Rotating Hairy Black Holes**  
Belhaj A., Chabab M., El Moumni H., Masmar K., Sedra M. B.
- 100501 Optimal Performance Analysis of a Three-Terminal Thermoelectric Refrigerator with Ideal Tunneling Quantum Dots**  
SU Hao, SHI Zhi-Cheng, HE Ji-Zhou
- 100701 A Longitudinal Zeeman Slower Based on Ring-Shaped Permanent Magnets for a Strontium Optical Lattice Clock**  
WANG Qiang, LIN Yi-Ge, GAO Fang-Lin, LI Ye, LIN Bai-Ke, MENG Fei, ZANG Er-Jun, LI Tian-Chu, FANG Zhan-Jun

## THE PHYSICS OF ELEMENTARY PARTICLES AND FIELDS

- 101101 Tunneling of Relativistic Bosons Induced by Magnetic Fields in the Magnetar's Crust**  
Marina-Aura Dariescu, Ciprian Dariescu, Denisa-Andreea MiHu
- 101201 Identification of  $Y(4008)$ ,  $Y(4140)$ ,  $Y(4260)$ , and  $Y(4360)$  as Tetraquark States**  
ZHOU Ping, DENG Cheng-Rong, PING Jia-Lun

## FUNDAMENTAL AREAS OF PHENOMENOLOGY(INCLUDING APPLICATIONS)

- 104201 High-Power Dual-End-Pumped Actively Q-Switched Ho:YAG Ceramic Laser**  
DUAN Xiao-Ming, YUAN Jin-He, YAO Bao-Quan, DAI Tong-Yu, LI Jiang, PAN Yu-Bai
- 104202 Light Focusing through Scattering Media by Particle Swarm Optimization**  
HUANG Hui-Ling, CHEN Zi-Yang, SUN Cun-Zhi, LIU Ji-Lin, PU Ji-Xiong
- 104203 High-Power and High-Efficiency Operation of Terahertz Quantum Cascade Lasers at 3.3 THz**  
LI Yuan-Yuan, LIU Jun-Qi, WANG Tao, LIU Feng-Qi, ZHAI Shen-Qiang, ZHANG Jin-Chuan, ZHUO Ning, WANG Li-Jun, LIU Shu-Man, WANG Zhan-Guo
- 104204 Polarization Stable Vertical Cavity Surface Emitting Laser Array Based on Proton Implantation**  
XUN Meng, XU Chen, XIE Yi-Yang, DENG Jun, XU Kun, JIANG Guo-Qing, PAN Guan-Zhong, CHEN Hong-Da
- 104205 Efficient Passively Q-Switched Nd:YAG/Cr<sup>4+</sup>:YAG/LBO Microchip Laser**  
FU Sheng-Gui, OUYANG Xue-Ying, LIU Xiao-Juan
- 104206 Surface Plasmon Interference Lithography Assisted by a Fabry-Perot Cavity Composed of Subwavelength Metal Grating and Thin Metal Film**  
LIANG Hui-Min, WANG Jing-Quan, WANG Xue, WANG Gui-Mei
- 104207 Attosecond-Resolution Er:Fiber-Based Optical Frequency Comb**  
YAN Lu-Lu, ZHANG Yan-Yan, ZHANG Long, FAN Song-Tao, ZHANG Xiao-Fei, GUO Wen-Ge, ZHANG Shou-Gang, JIANG Hai-Feng
- 104208 Cr<sup>2+</sup>:ZnS Saturable Absorber Passively Q-Switched Ho:LuVO<sub>4</sub> Laser**  
CUI Zheng, YAO Bao-Quan, DUAN Xiao-Ming, BAI Shuang, LI Jiang, YUAN Jin-He, DAI Tong-Yu, LI Chao-Yu, PAN Yu-Bai

- 104209 **Heptad Phase Vortex Array in Extremely Deep Fresnel Diffraction Region Generated by Asymmetrical Metal Subwavelength Holes Film**  
JIANG Shu-Na, LI Xing, MA Li, GAO Ya-Ru, GUI Wei-Ling, CHENG Chuan-Fu
- 104210 **Trapping and Cooling of Single Atoms in an Optical Microcavity by a Magic-Wavelength Dipole Trap**  
LI Wen-Fang, DU Jin-Jin, WEN Rui-Juan, LI Gang, ZHANG Tian-Cai
- 104401 **Thermal Transport in Methane Hydrate by Molecular Dynamics and Phonon Inelastic Scattering**  
WANG Zhao-Liang, YUAN Kun-Peng, TANG Da-Wei

### PHYSICS OF GASES, PLASMAS, AND ELECTRIC DISCHARGES

- 105201 **MF-DFA Analysis of Turbulent Transport Measured by a Multipurpose Probe**  
Lafouti M., Ghoranneviss M.

### CONDENSED MATTER: STRUCTURE, MECHANICAL AND THERMAL PROPERTIES

- 106101 **Magneto-Caloric Response of a  $Gd_{55}Co_{25}Al_{18}Sn_2$  Bulk Metallic Glass**  
DING Ding, ZHANG Yi-Qing, XIA Lei
- 106201 **External-Strain-Induced Raman Scattering Modification in  $g-C_3N_4$  Structures**  
LI Ting-Hui, LI Hai-Tao, PAN Jiang-Hong, GUO Jun-Hong, HU Fang-Ren
- 106801 **Growth and Characterization of  $InAs_{1-x}Sb_x$  with Different Sb Compositions on GaAs Substrates**  
SUN Qing-Ling, WANG Lu, WANG Wen-Qi, SUN Ling, LI Mei-Cheng, WANG Wen-Xin, JIA Hai-Qiang, ZHOU Jun-Ming, CHEN Hong

### CONDENSED MATTER: ELECTRONIC STRUCTURE, ELECTRICAL, MAGNETIC, AND OPTICAL PROPERTIES

- 107101 **Observation of Fermi Arcs in Non-Centrosymmetric Weyl Semi-Metal Candidate NbP**  
XU Di-Fei, DU Yong-Ping, WANG Zhen, LI Yu-Peng, NIU Xiao-Hai, YAO Qi, Dudin Pavel, XU Zhu-An, WAN Xian-Gang, FENG Dong-Lai
- 107301 **Transport through a Single Barrier on Monolayer  $MoS_2$**   
CHENG Fang, REN Yi, SUN Jin-Fang
- 107302 **Wet Chemical Etching of Antimonide-Based Infrared Materials**  
HAO Hong-Yue, XIANG Wei, WANG Guo-Wei, XU Ying-Qiang, REN Zheng-Wei, HAN Xi, HE Zhen-Hong, LIAO Yong-Ping, WEI Si-Hang, NIU Zhi-Chuan
- 107303 **Effect of Thermal Annealing on Light-Induced Minority Carrier Lifetime Enhancement in Boron-Doped Czochralski Silicon**  
WANG Hong-Zhe, ZHENG Song-Sheng, CHEN Chao
- 107304 **Contact-Size-Dependent Cutoff Frequency of Bottom-Contact Organic Thin Film Transistors**  
SUN Jing, WANG Hong, WANG Zhan, WU Shi-Wei, MA Xiao-Hua
- 107305 **Waveguide Mode Splitter Based on Multi-mode Dielectric-Loaded Surface Plasmon Polariton Waveguide**  
CAI Yong-Jing, LI Ming, XIONG Xiao, YU Le, REN Xi-Feng, GUO Guo-Ping, GUO Guang-Can
- 107401 **New Superconductivity Dome in  $LaFeAsO_{1-x}F_x$  Accompanied by Structural Transition**  
YANG Jie, ZHOU Rui, WEI Lin-Lin, YANG Huai-Xin, LI Jian-Qi, ZHAO Zhong-Xian, ZHENG Guo-Qing
- 107801 **Polarization Insensitivity in Double-Split Ring and Triple-Split Ring Terahertz Resonators**  
WU Qian-Nan, LAN Feng, TANG Xiao-Pin, YANG Zi-Qiang
- 107802 **Synthesis, Structure and Optical Properties of CdO Nanocrystals Directly Grown on Cd Foil**  
LI Yong, LING Hong, GAO Lei, SONG Yue-Li, TIAN Ming-Li, ZHOU Feng-Qun
- 107803 ***Ab Initio* Study of the Dynamical Si-O Bond Breaking Event in  $\alpha$ -Quartz**  
SU Rui, ZHANG Hong, HAN Wei, CHEN Jun

- 107804 Au Microdisk-Size Dependence of Quantum Dot Emission from the Hybrid Metal-Distributed Bragg Reflector Structures Employed for Single Photon Sources**  
WANG Hai-Yan, SU Dan, YANG Shuang, DOU Xiu-Ming, ZHU Hai-Jun, JIANG De-Sheng, NI Hai-Qiao, NIU Zhi-Chuan, ZHAO Cui-Lan, SUN Bao-Quan
- 107805 High-Performance Hybrid White Organic Light-Emitting Diodes Utilizing a Mixed Interlayer as the Universal Carrier Switch**  
DING Lei, LI Huai-Kun, ZHANG Mai-Li, CHENG Jun, ZHANG Fang-Hui
- 107901 Fabrication of Through Micro-hole Arrays in Silicon Using Femtosecond Laser Irradiation and Selective Chemical Etching**  
GAO Bo, CHEN Tao, CHEN Ying, SI Jin-Hai, HOU Xun

### **CROSS-DISCIPLINARY PHYSICS AND RELATED AREAS OF SCIENCE AND TECHNOLOGY**

- 108101 Simple Method to Fabricate Au Nanoparticle-Decorated TiO<sub>2</sub> Nanotube Arrays for Enhanced Visible Light Photocurrent**  
LU Yu-Hua, WANG Wen-Gui, WENG Yu-Yan, DONG Wen
- 108102 Fabrication and Piezoelectric Characterization of Single Crystalline GaN Nanobelts**  
WU Dong-Xu, CHENG Hong-Bin, ZHENG Xue-Jun, WANG Xian-Ying, WANG Ding, LI Jia
- 108501 High-Efficiency Bottom-Emitting Organic Light-Emitting Diodes with Double Aluminum as Electrodes**  
ZHANG Hong-Mei, WANG Dan-Bei, WU Yuan-Wu, FANG Da, HUANG Wei
- 108502 Statistical Modeling of Gate Capacitance Variations Induced by Random Dopants in Nanometer MOSFETs Reserving Correlations**  
LÜ Wei-Feng, WANG Guang-Yi, LIN Mi, SUN Ling-Ling
- 108503 Quantum Coupling Effect between Quantum Dot and Quantum Well in a Resonant Tunneling Photon-Number-Resolving Detector**  
WENG Qian-Chun, AN Zheng-Hua, XIONG Da-Yuan, ZHU Zi-Qiang
- 108701 Temperature Effects on Information Capacity and Energy Efficiency of Hodgkin–Huxley Neuron**  
WANG Long-Fei, JIA Fei, LIU Xiao-Zhi, SONG Ya-Lei, YU Lian-Chun
- 108702 Improvements for Manipulating DNA with Optical Tweezers**  
ZHU Chun-Li, LI Jing

### **GEOFYSICS, ASTRONOMY, AND ASTROPHYSICS**

- 109501 Quintessence Cosmology with an Effective  $\Lambda$ -Term in Lyra Manifold**  
Khurshudyan M., Pasqua A., Sadeghi J., Farahani H.

JUST FOR AUTHORS  
— CHINESE PHYSICS LETTERS